

1 Title: **Locating primary somatosensory cortex in human brain stimulation**
2 **studies: Experimental evidence**

3

4 Running head: Locating S1 in human brain stimulation studies

5

6 Authors: Nicholas Paul Holmes¹, Luigi Tamè², Paisley Beeching¹, Mary Medford³,
7 Mariyana Rakova³, Alexander Stuart¹, Silvia Zeni¹

8

9 Affiliations:

10 1. School of Psychology, University of Nottingham, University Park, Nottingham, UK.

11 ORCID: 0000-0001-9268-4179; npholmes@neurobiography.info

12 2. Department of Psychological Sciences, Birkbeck University of London, London,

13 UK. ORCID: 0000-0002-9172-2281

14 3. School of Psychology and Clinical Language Sciences, University of Reading,

15 Reading, UK.

16

17 Author contributions:

18 Collected data: NPH, LT, PB, MM, MR, AS

19 Analysed data: NPH, LT, PB, AS, SZ

20 Wrote the paper: NPH

21 Commented on the paper: LT, PB, MM, MR, AS, SZ

22

23 Acknowledgements: This work was supported by the Medical research Council [grant

24 number MR/K014250/1 to NPH].

25 **Abstract**

26 Transcranial magnetic stimulation (TMS) over human primary somatosensory cortex
27 (S1) does not produce immediate outputs. Researchers must therefore rely on
28 indirect methods for TMS coil positioning. The 'gold standard' is to use individual
29 functional and structural magnetic resonance imaging (MRI) data, but the majority of
30 studies don't do this. The most common method to locate the hand area of S1 (S1-
31 hand) is to move the coil posteriorly from the hand area of primary motor cortex (M1-
32 hand). Yet, S1-hand is not directly posterior to M1-hand. We localised the index finger
33 area of S1-hand experimentally in four ways. First, we re-analysed functional MRI
34 data from 20 participants who received vibrotactile stimulation to their 10 digits.
35 Second, to assist the localisation of S1-hand without MRI data, we constructed a
36 probabilistic atlas of the central sulcus from 100 healthy adult MRIs, and measured
37 the likely scalp location of S1-index. Third, we conducted two experiments mapping
38 the effects of TMS across the scalp on tactile discrimination performance. Fourth, we
39 examined all available neuronavigation data from our laboratory on the scalp location
40 of S1-index. Contrary to the prevailing method, and consistent with systematic review
41 evidence, S1-index is close to the C3/C4 electroencephalography (EEG) electrode
42 locations on the scalp, approximately 7-8 cm lateral to the vertex, and approximately
43 2 cm lateral and 0.5 cm posterior to the M1-FDI scalp location. These results suggest
44 that an immediate revision to the most commonly-used heuristic to locate S1-hand is
45 required. The results of many TMS studies of S1-hand need reassessment.

46 **New and noteworthy**

47 Non-invasive human brain stimulation requires indirect methods to target particular
48 brain areas. Magnetic stimulation studies of human primary somatosensory cortex
49 have used scalp-based heuristics to find the target, typically locating it 2cm posterior
50 to the motor cortex. We measured the scalp location of the hand area of primary
51 somatosensory cortex, and found that it is approximately 2 cm lateral to motor cortex.
52 Our results suggest an immediate revision of the prevailing method is required.

53

54 Keywords: S1, SI, TMS, TDCS, vibrotactile

55 1. Introduction

56 Transcranial magnetic stimulation (TMS, Barker et al. 1985) can be used to study the
57 healthy human brain non-invasively, by stimulating brain tissue electromagnetically.
58 TMS therefore requires indirect methods of locating the brain area of interest.
59 Primary motor cortex (M1) can be located relatively easily, by moving the TMS coil
60 around on the scalp, applying single pulses of TMS, and observing or recording
61 muscle responses, however, for most other brain areas, there is no similar,
62 immediate and objective output that researchers can use, on a pulse-by-pulse basis,
63 to ensure correct TMS coil position. The 'gold standard' in this field is to acquire, for
64 every participant, structural and functional brain imaging data and use frameless
65 stereotaxy (Sparing et al. 2010).

66

67 When MRI is not available, researchers have used scalp-based heuristics to target
68 the hand area of primary somatosensory cortex (S1-hand, Holmes & Tamè, in press;
69 preprints available at: <https://osf.io/c8nhj/>). These heuristics have included using the
70 10-20 or 10-10 electroencephalographic system (Jasper 1958; Koessler et al. 2009;
71 Lagerlund et al. 1993; Okamoto et al. 2004; Towle et al. 1993; Vitali et al. 2002; Xiao
72 et al. 2018), functionally-identified scalp locations for motor cortex (e.g., Balslev et al.
73 2004), changes in reaction times or errors (e.g., Convento et al. 2018), or changes in
74 sensation (e.g., Sugishita & Takayama 1993; Cowey & Walsh 2000). Systematic
75 review revealed the most common heuristic involves positioning the coil 2 cm
76 posterior to the M1 representation of hand muscles (e.g., first dorsal interosseus,
77 FDI, or abductor pollicis brevis, APB), yet S1-hand is lateral, not posterior to M1-hand
78 (Holmes & Tamè, in press). In previous work using individual fMRI-guided

79 neuronavigation (Tamè & Holmes, 2016), we noticed that, in all 20 of our participants,
80 the scalp location above S1-index was indeed lateral, not directly posterior, to M1.

81

82 Here, we ask: “what is the optimal location on the scalp to magnetically stimulate the
83 somatosensory cortex (Brodmann's areas BA3b & BA1, Geyer et al. 1999)

84 representations of the index finger (S1-index)? The index finger and the FDI muscles
85 are the most commonly stimulated and recorded body parts in the relevant literature,

86 respectively, so we focused on them. We focused on the BA3b and BA1 subregions

87 of S1 because they show a clear somatotopy for individual fingers (Nelson & Chen

88 2008), because our fMRI protocol was not able to distinguish between them, and, for

89 the purposes of applying TMS on the scalp, because the representations of each

90 finger in BA3b and BA1 lie very close to each other (e.g., Figure 2 in Holmes & Tamè,

91 in press). We answered the question in four ways: First, by re-analysing functional

92 MRI data from our laboratory (Tamè & Holmes, 2016); Second, by creating a

93 probabilistic atlas of the central sulcus from 100 structural MRIs, and measuring

94 between-participant variability in central sulcus location at the likely position of S1-

95 index; Third, by conducting two experiments which systematically mapped the effect

96 of TMS on vibrotactile discrimination performance across the scalp, and; Fourth, by

97 summarizing all our available data from individual (F)MRI-neuronavigated TMS

98 experiments targeting S1-index. Together, these independent and converging lines of

99 evidence strongly support the immediate revision of the most commonly-used

100 heuristic for locating human primary somatosensory cortex in TMS studies.

101

102

Materials and methods

Studies were approved by research ethics committees (UREC11/58, University of Reading, UK; SoPEC916, University of Nottingham, UK), conducted in accordance with TMS safety guidelines (Rossi et al. 2009) and the Declaration of Helsinki (2008 version, which does not require pre-registration).

Participants

FMRI experiment: Twenty healthy participants (mean \pm SD age=27.6 \pm 8.7 years, 15 female, 3 left-handed by self-report). Structural MRI: 100 right-handed participants (mean \pm SD age=25.1 \pm 6.2 years, 64 female; Holmes et al., 2008; Tamè and Holmes, 2016, unpublished datasets). Experiment 1: nine participants (mean \pm SD age=33.2 \pm 11.6 years, 5 female, 1 ambidextrous; 13 were recruited, 4 were removed). Experiment 2: twelve participants (mean \pm SD age=23.7 \pm 5.6 years, 5 females, 12 right-handed). Participants met TMS safety inclusion criteria (Rossi et al. 2009), with no neuropsychiatric disorder. Neuronavigation: 37 localisations of S1-index from 15 participants, separately for left (N=11, mean \pm SD=25.4 \pm 6.1 years, 7 female) and right hemispheres (N=9, mean \pm SD=26.2 \pm 6.3 years, 3 female).

Functional MRI data

Data reported by Tamè and Holmes (2016) were re-analysed. Participants underwent 10x280 s scans, each comprising 10x11.5 s vibrotactile stimulation blocks interleaved with 10x12.5 s rest. Stimuli were produced by MRI-compatible piezoelectric wafers driving a 2.5 mm diameter plastic rod (~100Hz, 8x1 s, 0.5 s pause). One scan (Siemens Trio 3T, 3x3x3 mm) was collected for each digit on each hand, in

127 pseudorandomised order. FMRI data were processed with FSL5
 128 (<http://www.fmrib.ox.ac.uk/fsl>): 3D spatial smoothing (5 mm FWHM), 6- and 12-
 129 degree-of-freedom linear registration to the anatomical (MPRAGE, 1x1x1 mm) and
 130 MNI152 (2x2x2 mm) template brains, respectively. Data were modeled as square-
 131 wave regressors convolved with canonical hemodynamic response functions. Two
 132 contrasts were made with each set of 10 scans: Single digit contrasts of vibration
 133 versus rest, within scans; Differential contrasts of each digit against the other four of
 134 that hand, across scans (e.g., left index finger (D2) contrasted against the left thumb
 135 (D1), middle (D3), ring (D4), and little (D5) digits, weights: [-1,4,-1,-1,-1]). Group
 136 means were calculated for each digit and each contrast (20 group-level images). The
 137 voxel with maximum Z-score in postcentral gyrus of presumed primary
 138 somatosensory cortex of each group image was recorded. Harvard-Oxford and
 139 Juelich atlases (Eickhoff et al. 2005) within FSLView were used to assign probabilistic
 140 anatomical and functional labels to voxels.

141

142 ***Probabilistic atlas of the central sulcus, and S1-index scalp location***

143 Structural MRI scans were used to create a probabilistic central sulcus atlas. The
 144 location of S1-index on the scalp was estimated by measuring seven points along the
 145 scalp between midline and the scalp overlying S1-index (MNI[-48,-21,50], Holmes &
 146 Tamè, in press). 112 scans (MPRAGE, 1x1x1 mm) were acquired from: Siemens
 147 Sonata 1.5T (N=43, University of Oxford, UK); Siemens Magnetom Trio 3T (N=20,
 148 University of Reading, UK), and Philips Achieva 3T (N=49, University of Nottingham,
 149 UK). 8 were excluded for self-reported left-handedness, 1 for scan quality (artefacts),
 150 and 1 for poor health (severe uncorrected visual deficits). 2 scans which did not

151 include the full scalp, nasion, and inion were also removed.

152

153 Each image was viewed in axial/transverse plane, by NPH or SZ. Using a 2 mm

154 'pencil', the complete bilateral course of the central sulcus was drawn on the image,

155 starting at the hand knob, moving superiorly then inferiorly and laterally from the hand

156 area. We filled all gaps between pre- and postcentral gyri to provide a liberal estimate

157 of central sulcus location and width. Five landmarks were drawn on the images with

158 3x3x3 mm masks: nasion, inion, left and right pre-auricular points, vertex (Figure 1H).

159 Nasion and pre-auricular points were easily identified, but inion prominence varied

160 greatly. Vertex was estimated by calculating a line orthogonal to and through the

161 intersection of nasion-inion and pre-auricular lines, then using ruler and protractor to

162 find the scalp location 90 degrees from the intersection. A best guess for vertex

163 location was then taken, considering three image planes. It is not known how these

164 locations correspond to those measured on participants' heads during S1-index TMS.

165

166 Participants' brain images were extracted using BET, and both head and brain were

167 registered to MNI152 1x1x1 mm templates using FLIRT (12 degrees of freedom). The

168 two transformations (head, brain) were applied to central sulcus mask images to

169 create masks in standard MNI space. 100 masks were summed to create a

170 probabilistic atlas of the central sulcus where voxel intensity is the percentage of

171 participants with central sulcus passing through.

172

173 S1-index location was estimated relative to vertex using a mask of meta-analytic

174 mean MNI coordinates for S1-index (MNI[-48,-21,50]), transformed into

175 scanner/anatomical space per MRI. To account for non-alignment between head and
176 scanner axes, nasion, inion, and vertex on each image were used to form a plane,
177 NIV (i.e., mid-sagittal). The nearest voxel to S1-index on the scalp was estimated,
178 and projected orthogonally onto NIV. This projection was used to generate six pairs of
179 coordinates (x,y) between S1-index and NIV. Each pair's Z-coordinate was recorded
180 as the most superior scalp voxel where x- and y-coordinates matched the projection.
181 Distances between adjacent points, and the distance between S1-index and vertex
182 were calculated. For anterior distances, the y-coordinate of the S1-index projection
183 onto NIV was subtracted from the vertex y-coordinate and divided by the cosine of
184 the angle between nasion-inion and scanner y-axis.

185

186 ***Experiment 1: Mapping effects of TMS on tactile discrimination thresholds***

187 Participants trained to detect and discriminate vibrotactile stimuli (150 Hz, 50 ms,
188 Oticon bone-conductor) on their right index finger. The first training was 48 trials of 2-
189 interval forced choice (2IFC) detection, in which a pseudorandom interval contained a
190 target. 1s intervals were preceded by a 250 ms light emitting diode (LED) flash on the
191 left (first) or right (second interval). Targets were presented mid-interval, and were
192 followed by a 2.5 s response period. Participants released a pedal under their left
193 (indicating the target was in the first) or right foot (second interval). Incorrect
194 responses were followed by 2x250 ms flashes from both LEDs. Trials were separated
195 by 1 s. Target intensity began at 0.8 (arbitrary units), adjusted by QUEST (Watson
196 and Pelli, 1983) implemented in PsychToolBox3 (Brainard, 1997). The second
197 training was 2IFC intensity discrimination. One interval contained a 'weak' (1.5x
198 detection threshold), the other a 'strong' vibration (starting at 1.8x weak intensity).

199 Participants responded with left feet for strong (targets) in the first, and right for the
200 second interval. Threshold for 2IFC tasks was ~76 % correct, taken as the final trial's
201 value of QUESTMean. The third training was 1IFC intensity discrimination. Half the
202 intervals contained a weak (1.5x detection threshold), and half a strong vibration
203 (starting at 1.8x weak intensity). Participants classified stimuli as 'strong' (left) or
204 'weak' (right pedal). The strong intensity was adjusted with QUEST. Threshold was
205 69 % correct (equivalent to 76 % in 2IFC). A single pulse of TMS at 50 % maximum
206 stimulator output (MSO) was presented ~30 cm away from the participant's head, 25
207 ms after the onset of each vibration.

208

209 We refer to scalp and brain coordinates thus: ORIGIN(lateral, anterior). Right and
210 anterior are positive, left and posterior negative. For example, 5 cm left and 1 cm
211 anterior to vertex: Cz(-5,1); 2 cm posterior to the optimal FDI location: FDI(0,-2). MNI
212 neuroimaging coordinates are: MNI(X,Y,Z), in mm. Resting motor threshold (RMT) for
213 the FDI was estimated using motor evoked potentials (MEPs) in the electromyograph
214 (EMG, AD Instruments Powerlab 16/30; BioAmplifier, silver/silver-chloride electrodes
215 over FDI belly and distal second metacarpal, Criswell, 2011; monophasic Magstim
216 200^2 BiStim module, standard BiStim mode, figure-of-8, 100 mm outer diameter
217 coil). Test pulses ~5-10 s apart were presented while the coil was moved around, at
218 approximately Cz(-5,1), starting at 50 % MSO, increasing and decreasing to find the
219 threshold (i.e., 5/10 trials with minimum peak-to-peak MEP amplitude of 50 μ V, both
220 peaks within 20-60 ms). The coil handle pointed posterolaterally, approximately 45
221 degrees to the midline; current anterior-to-posterior.

222

223 The mapping experiment was 10 blocks of 48 trials of 1IFC intensity discrimination,
224 with TMS at one of 10 pseudorandomly ordered locations (Fig. 1F, white circles). A
225 grid of ten locations was placed on participants' heads, with the origin, location 2,
226 L2=FDI(0,0). The 9 other locations were: L1=FDI(+2,-2), L3=FDI(0,-2), L4=FDI(0,-4),
227 L5=FDI(-2,+2), L6=FDI(-2,0), L7=FDI(-2,-2), L8=FDI(-2,-4), L9=FDI(-4,0), and
228 L10=FDI(-4,-2).

229

230 Two participants (#3, #8) could not perform training. Two participants (#10, #12)
231 performed poorly with TMS (i.e., floor effects, QUEST reached ceiling) on 8 blocks.
232 #7 showed floor effects on six, #11 on two, and #5, #6, and #9 on one block each.
233 Floor effects reduce variability at lower performance ranges (Holmes, 2009). A
234 scatterplot of participants' across-block means against across-block SDs revealed
235 two outliers (#10, #12), with low coefficient of variation (SD/mean). These participants
236 were removed; the reported mean effects of TMS are therefore likely under-
237 estimated.

238

239 ***Experiment 2: Controlling for non-specific effects of TMS***

240 Experiment 1 contained one task and 10 locations. Changes in performance across
241 locations could be due to differences in TMS-related discomfort rather than effects on
242 the brain (Meteyard & Holmes, 2018; Holmes & Meteyard 2018; [http://tms-](http://tms-smart.info)
243 [smart.info](http://tms-smart.info)). Experiment 2 improved TMS localization and participant performance.
244 Participants also performed auditory intensity discrimination to control for non-specific
245 TMS effects.

246

247 EMG data were recorded from electrodes over FDI and flexor digitorum superficialis
 248 (FDS; Criswell, 2011). M1 was systematically mapped at 20 grid locations oriented
 249 ~45 degrees to midline (Fig. 1A, white circles). During discrimination, seven TMS
 250 locations were stimulated (4x2 grid, 2 cm spacing). An extra location was added, at
 251 FDI(-1,-1), as our best guess (at the time) of optimal S1-index location: L1=FDI(0,0),
 252 L2=FDI(0,-2), L3=FDI(-1,-1), L4=FDI(-2,0), L5=FDI(-2,-2), L6=FDI(-4,0), and
 253 L7=FDI(-4,-2), see Fig. 1C (white circles). Participants performed two
 254 counterbalanced 1IFC intensity discrimination tasks (vibrotactile, auditory). In
 255 auditory blocks, a speaker was positioned near participants' hands. Target frequency
 256 was 200 Hz. Weak intensity was 2x detection threshold, strong was 1.5x
 257 discrimination threshold above the weak intensity. 20 trials with fixed intensity were
 258 used. Based on unpublished data, TMS was triggered 50 ms after stimulus onset
 259 (i.e., approximately mid-way through stimulus processing, assuming ~25ms
 260 conduction time). A 75 mm outer diameter TMS coil was used.
 261
 262 Participants' heads were measured. Five pulses of TMS were presented at each of
 263 20 locations on the 5(medial-lateral)x4(anterior-posterior) grid (Figure 1A, white
 264 circles), with 1 cm spacing, centered on Cz(-5,1). The mean MEP amplitude across 5
 265 trials at each location was recorded. The 20 locations were tested sequentially,
 266 starting anteromedially, #1, Cz(-3,2.5), proceeding posterolaterally to #4, Cz(-3,-0.5),
 267 then #5, Cz(-4,2.5), finishing at #20, Cz(-7,-0.5). The location with maximal mean
 268 MEP amplitude per participant was designated M1-FDI; RMT was measured here.
 269
 270 Participants performed tactile and auditory tasks in two counterbalanced ~60 minute

271 sessions. Two training tasks were performed per session: 2IFC detection, 2IFC
272 intensity discrimination. The experiment included seven blocks of 20 trials, each with
273 TMS over one pseudorandomised location. Data were analyzed as proportion
274 correct, $d\text{-prime} = Z(\text{Hits}) - Z(\text{False alarms})$, and $\text{criterion} = -0.5 * (Z(\text{Hits}) + Z(\text{False}$
275 $\text{alarms}))$, Tamè & Holmes, 2016). The coil was held at ~45 degrees to midline, handle
276 posterolaterally, current anterior-to-posterior.

278 ***Scalp measurements of S1-index***

279 The scalp locations of S1-index across all our available neuronavigated TMS data
280 from nine unpublished experiments were summarised. For all measurements we had
281 a recent structural MRI scan, and used atlas coordinates derived either from
282 individual fMRI data, from group (N=20) fMRI data, or from meta-analysis (Holmes
283 & Tamè, in press). All available sources of information were used. The target was on
284 the anterior bank and/or crown of postcentral gyrus. Anatomical criteria (i.e., over
285 postcentral gyrus, posterior to central sulcus) were prioritised over fMRI data. fMRI
286 coordinates, whether based on individual, group, or meta-analysis, indicated that S1-
287 index was, in every participant, lateral to or on the lateral border of the precentral
288 gyrus 'hand knob' (Yoursy et al., 1997).

290 ***Analytic strategy***

291 This report provides multiple independent estimates of the optimal scalp location to
292 stimulate S1-index. The analysis was largely exploratory, to estimate rather than
293 hypothesis-test. Means and SDs are given for distances, locations, and TMS
294 parameters; means and standard errors (SE) are given for behavioral performance,

muscle responses, and between condition differences, where statistical comparisons are made. Our experimental question is: are there consistencies in optimal TMS location across the samples typically used in similar TMS experiments ($N \approx 12$). Reported p-values are uncorrected, unless otherwise stated. We believe minimizing sample size is important for human brain stimulation experiments, to reduce the risk that TMS poses - three of our participants have suffered syncope or fainting (Reader et al., 2017). Our approach is therefore to search for large, consistent effects (Smith & Little, 2018), and accumulate multiple, independent, converging sources of evidence. Where statistical tests are used, we are comfortable with the conventional long-run false positive error rate of 5 % (Lakens et al. 2018). Data, scripts, and previous versions of our work are freely available at <https://osf.io/c8nhj/>.

306

307 **Results and statistical analyses**

308 *Functional MRI data.* The group peak voxel locations and probabilistic anatomy for BOLD responses to vibrotactile stimulation of ten digits are in Table 1. The data are unable to resolve different S1 subregions, so only peak S1 voxels are reported. The differential contrasts, of each digit against the other four, resulted in lower BOLD Z-scores (across-digit mean \pm SD $Z=2.69\pm0.86$) than single condition contrasts (mean \pm SD $Z=4.14\pm0.65$), as expected – the single contrasts do not account for general task-related or finger non-specific activity common to all conditions in contrast with rest. The peak voxels in the two contrasts were mean \pm SD 5.44 ± 4.05 mm apart. Left hemisphere peak voxel locations ranged superiorly from MNI(-40,-30,64) for the little, to MNI(-50,-18,44) for the index; right hemisphere ranged from MNI(40,-30,66) for the ring, to MNI(56,-12,46) for the index finger. The peak

319 differential contrast voxels for S1-index were MNI(-48,-14,50) for left, and MNI(48,-
320 12,54) for right hemisphere.

321

322 *Probabilistic atlas of the central sulcus, and S1-index scalp location.* The 100 central
323 sulcus masks were summed into a single image, indicating the percentage of
324 participants whose central sulcus included each voxel (Fig. 1B, left panel). The brain
325 registration was less variable than the head registration (Fig. 1B, right panel). The
326 between-participant range in Y-axis position of the central sulcus at the level of S1-
327 index, MNI(-48,-21,50), was around 2-3 cm. The mean \pm SD location of S1-index
328 projected onto the scalp was 6.8 \pm 0.4 cm lateral and 0.6 \pm 0.7 cm posterior to the
329 vertex (Fig. 1B, 1D, 1E, blue square; Table 2).

330

331 *Experiment 1: Mapping effects of TMS on tactile discrimination thresholds.* In training,
332 nine participants' mean \pm SE 2IFC detection threshold was 0.473 \pm 0.105 (A.U.); 2IFC
333 discrimination threshold was 1.50 \pm 0.09 times weak intensity (1.71 \pm 0.26 dB, D'Amour
334 and Harris 2014; Tamè et al. 2014); and 1IFC discrimination threshold was 1.52 \pm 0.15
335 times weak intensity (1.64 \pm 0.41 dB). Mean \pm SD RMT=44.3 \pm 4.9 % MSO. TMS was
336 applied at mean \pm SD=119 \pm 1.7 % RMT (mean \pm SD=52.7 \pm 5.3 % MSO). Due to
337 researchers not recording data, scalp locations for M1-FDI were available for only
338 seven participants, with mean \pm SD Cz(6.0 \pm 1.0,0.9 \pm 0.6) cm. Overall mean \pm SE
339 discrimination threshold across 10 locations was 2.73 \pm 0.26 dB (Fig. 1F), with best
340 performance (2.3 \pm 0.4 dB) at FDI(0,-2), and worst (3.36 \pm 0.31 dB) at FDI(-2,2) (Fig.
341 1D, 1F, black cross). Thresholds were higher (worse) than in training, with locations
342 5, 6, and 9 significantly (.012 \leq p \leq .032). Pairwise comparisons between all 10 sites

revealed significant differences between FDI(-2,2), and locations 2, 3, 4, 6, 8, and 10 (.026≤p≤.049). Across locations, mean±SE MEPs were 0.178±0.039 mV, from 0.106±0.027 mV at FDI(0,-4), to 0.439±0.186 mV at FDI(0,0). Within-participant correlations between MEP amplitude and discrimination threshold across 10 locations varied from r(8)=-0.499 to r(8)=.417 (uncorrected two-tailed ps>.14). R-values were converted to Z-scores to allow parametric analysis; across participants, mean±SE Z-score was small (0.100±0.110, t(8)=0.905, p=.389).

Experiment 2: Controlling for non-specific effects of TMS. Training performance on 2IFC detection was mean±SE=0.0483±0.0112 (A.U.) for tactile, and 0.0319±0.0029 for auditory stimuli, t(11)=0.145, p=.887. 2IFC intensity discrimination performance was 0.352±0.055 (1.27±0.16 dB) for tactile, and 0.524±0.113 (1.71±0.30 dB) for auditory, t(11)=.876, p=.160. Participants' head sizes were a mean±SD=38.0±2.3 cm from nasion-inion, and 36.5±1.8 cm between pre-auricular points. Across locations, mean±SE MEP amplitude=0.197±0.056 mV, from 0.003±0.002 mV at Cz(-5.4,3.5), to 0.526±0.283 mV at Cz(-6.1,-0.1) (Fig. 1A). Locations 3, 6, 9-11, and 15 produced MEPs significantly greater than zero (.005≤p≤.020). Pairwise comparisons revealed no clear pattern of differences. Across participants, Cz(-4.7,-1.5), Cz(-3.9,2.1), Cz(-4.7,1.4), Cz(-5.4,2.1), and Cz(-6.8,0.7) produced maximal MEPs in one participant, Cz(-3.2,1.4) and Cz(-6.1,-0.1) in two, and Cz(-5.4,0.7) in three. Mean±SD optimal location was Cz(-5.0±1.1,0.8±1.0). Mean±SD RMT at this site was 40.4±7.0%MSO.

TMS was presented during the experiment at a mean±SD of 120±0.6% RMT (48.4±8.4% MSO). Performance was worse with tactile (mean±SE d-

367 prime= 1.06 ± 0.12) than auditory targets (1.61 ± 0.2 , $t(11)=2.78$, $p=.018$). Response
 368 biases (tendency to respond 'stronger') were negligible, and comparable between
 369 touch (mean \pm SE criterion= -0.005 ± 0.039) and audition (0.055 ± 0.054 , $t(11)=0.938$,
 370 $p=.369$). Effects of TMS were assessed by differences between auditory and tactile
 371 tasks per location. TMS over FDI(-2,0) resulted in the largest decrement in
 372 performance (tactile mean \pm SE $d'=1.05 \pm 0.30$ vs. auditory= 1.93 ± 0.30 , mean \pm SE
 373 difference= 0.880 ± 0.265 , $t(11)=3.32$, $p=.007$), with FDI(0,0) second largest
 374 (0.942 ± 0.194 vs. 1.73 ± 0.346 , difference= 0.788 ± 0.318 , $t(11)=2.48$, $p=.031$, Fig. 1C,
 375 1D black 'target'; Table 2). All other sites showed worse performance for tactile
 376 targets, but none significantly. None of the response biases differed between auditory
 377 and tactile tasks, but participants were more likely to report 'weaker' tactile targets
 378 with TMS over FDI(0,0) (mean \pm SE criterion= $-.136 \pm 0.075$), than FDI(-2,0)
 379 (0.120 ± 0.087 , $t(11)=2.39$, $p=.036$), or FDI(-2,-2) (0.130 ± 0.110 , $t(11)=2.26$, $p=.045$).
 380
 381 MEPs were recorded from FDI and FDS, were monitored during experiments, but
 382 data were saved only for eight participants (#5-12). During the tactile task, mean \pm SE
 383 MEPs were smallest at FDI(-4,0) (FDI= 0.058 ± 0.026 mV) and FDI(-2,-2)
 384 (FDS= 0.014 ± 0.010 mV) and largest at FDI(0,0) (FDI= 1.51 ± 0.49 mV, FDS= 1.22 ± 0.43
 385 mV). During the auditory task, MEPs were smallest at FDI(-2,-2) (FDI= 0.01 ± 0.01 mV;
 386 FDS= 0.01 ± 0.01 mV) and largest at FDI(0,0) (FDI= 0.79 ± 0.29 mV, FDS= 0.55 ± 0.21
 387 mV). The smallest 'MEPs' (~ 0.01 mV) were not different from zero, much lower than
 388 the MEP threshold, and likely reflect electrical noise. Comparing auditory and tactile
 389 tasks, MEPs were not significantly different at any location. There were no significant
 390 correlations between performance (d') and MEP amplitude, either for tactile or

391 auditory tasks alone, the differences between them, for either muscle, or for both
392 muscles combined (nine comparisons on Z-scores, all $t(7) \leq 1.75$, all uncorrected
393 $p \geq .125$).

394

395 *Scalp measurements of S1-index.* The mean \pm SD scalp location of S1-index was Cz(-
396 $8.0 \pm 0.9, -0.4 \pm 1.0$) (left hemisphere, Fig. 1D, magenta circle; Table 2), and
397 Cz($8.4 \pm 1.1, -0.4 \pm 0.5$) (right hemisphere). Combining hemispheres across 15
398 participants, S1-index was at Cz($\pm 8.1 \pm 1.0, -0.3 \pm 0.8$). For seven participants,
399 mean \pm SD S1-index was at FDI($\pm 2.4 \pm 1.0, -0.5 \pm 1.3$).

400

401 **Discussion**

402 Re-analysis of fMRI data revealed the peak voxel for right index finger was very
403 close to the meta-analytic mean location of S1-index in BA3b and BA1. The
404 probabilistic central sulcus atlas revealed a 2-3 cm anterior-posterior range in central
405 sulcus location at the level of S1-index. This implies that researchers using template
406 MRI to position TMS coils are likely to make Y-axis errors of several cm in locating
407 the central sulcus. Projected onto the scalp, S1-index is 7 cm lateral, and 0.5 cm
408 posterior to vertex. These distances are likely to be slight underestimates, given that
409 participants typically have hair (not visible on MRI), and a bathing or EEG cap
410 between scalp and TMS coil. This underestimation is between 0.2 and 1.0 cm (Table
411 2). In Experiment 1, the location of maximal interference of TMS with tactile intensity
412 discrimination thresholds was 2 cm lateral, and 2 cm anterior to M1-FDI. Experiment
413 1, however, is relatively weak: two participants could not complete the task, two were
414 removed, and the statistical tests did not pass conservative multiple comparison

415 corrections. Instead, Experiment 2 provides strong evidence that maximal
416 interference with tactile intensity discrimination is 2 cm lateral to M1-FDI. Experiment
417 2 allows greater confidence that M1-FDI was optimally localized and that tactile
418 interference was due to a specific worsening of tactile relative to auditory
419 discrimination. Conservative correction for multiple comparisons revealed that the
420 only significant effect of TMS on tactile intensity discrimination was 2 cm lateral to
421 M1-FDI.

422

423 The more anterior location found in Experiment 1 than 2 may be due to the different
424 tasks used (threshold estimation vs. discrimination); to between-participant
425 differences in central sulcus anatomy or head shape; to variability in the precision of
426 our TMS methods and head measurements; or to increased TMS-related discomfort
427 at the most anterior site in Experiment 1 (Meteyard & Holmes, 2018; Holmes &
428 Meteyard, 2018). Experiment 2 included a control task so that TMS-related
429 discomfort was matched, and task-related differences were the dependent variable.
430 Without independent MRI evidence, the most likely cause is measurement error and
431 increased TMS-related discomfort at the most anterior site in Experiment 1.

432

433 Here, we reported multiple independent lines of evidence (Table 2, Figure 1) which
434 supports findings from a recent systematic review (Holmes & Tamè, in press): the
435 optimal location for stimulating the hand area of primary somatosensory cortex, on
436 average, is ~2 cm lateral, and ~0.5 cm posterior to M1-FDI. This finding of S1-hand
437 being more lateral than M1-hand is consistent with studies in which both M1-hand
438 and S1-hand are measured together (e.g., Blatow et al. 2011), and with the work of

Seyal and colleagues (1997), who systematically mapped TMS effects on tactile detection and discrimination at 25 locations in a grid centered on M1-hand. They found maximal interference when the TMS coil was 4 cm lateral and 0-2 cm posterior to M1-hand (Figure 2a and 2b in Seyal et al. 1997).

Assuming previous TMS studies found M1-FDI/APB in a similar location to our data, these results imply that TMS studies targeting S1-index have been, on average, 2.25 cm away from their target (Table 1). This is not a trivial distance. The mean figure-eight TMS coil used in these studies has a 7.5 cm outer wing diameter, implying an error of 30% of coil diameter. This is likely to impede stimulation effectiveness. TMS over motor cortex is sensitive to coil position changes of a few millimeters (e.g., Raffin et al., 2015). These large distances between the likely location of S1-index, and the locations targeted in prior experiments may explain why otherwise well-designed experiments may fail to interfere significantly with tactile perception (e.g., Convento et al. 2018, reviewed by Holmes and Tamè, 2018). Below, we discuss possible sources of variability in stimulating S1 using TMS.

Sources of variability in stimulating S1

Variability in TMS studies arises from participants, experimenters, and procedures. Participant-associated variability includes head size and shape (Zilles et al. 2002; Xiao et al. 2018), brain area size, shape, folding, location, and function. Experimenter-associated variability arises from the selection, measurement, and registration of anatomical landmarks and reference points (nasion, inion, vertex), and the positioning and orientation of the coil. Procedure-associated variability includes

the target, timing, intensity, orientation, waveform, frequency, and orientation of TMS.

We were surprised by the large within-participant and between-session/experimenter variability during our studies. This variability may explain the potentially surprising finding of Experiment 1, with maximal thresholds 2 cm lateral and 2 cm *anterior* to M1-FDI. Measurements on the scalp varied, laterally and anteriorly, by 3-4 cm between participants for M1-FDI relative to vertex (Niskanen et al. 2010), S1-index relative to vertex, and S1-index relative to M1-FDI. In part, this is due to errors in scalp measurement, MRI registration, and locating M1-FDI. In large part, however, it likely reflects between participant anatomical differences. Better training, communication, and day-to-day practice will minimize experimenter error; better understanding of M1-hand and S1-hand are required to optimise TMS protocols. Given the potential sources of variability in stimulating S1, we recommend consistent, systematic, and numerical reporting of every aspect and stage of TMS studies (Rossi et al. 2009; Rossini et al. 1994, 2015; Chipchase et al. 2012). This should be done for all studies, regardless of whether neuronavigation was used.

Limitations

Our approach relied on numerous sources of information which, we argued, converged on the result that S1-index is 2 cm lateral to M1-FDI. Despite this convergence, one might question whether meta-analysis of reported fMRI coordinates, or averaging fMRI data across participants is sufficient. We cannot distinguish between Brodmann's area BA3b, BA1, or BA2 with our fMRI data, as our localizers were not sufficiently powerful. Similar limitations may apply to our TMS

data (Fox et al. 2004). We also cannot account for biases intrinsic to fMRI – the data rely on oxygenation changes rather than neural activity, and may be biased by non-neural structures (Schweissfurth et al., 2014). Further, single peak voxel coordinates derived from multiple studies and participants do not reflect the likely extent of S1 activation following index finger stimulation, nor the total S1 territory involved. Better methods to estimate the optimal scalp location for S1-index TMS may be to combine probabilistic maps of S1 with the likelihood of TMS, accounting for individual brain anatomy (Petrov et al. 2017). The overlap or convolution of these probabilistic maps might provide more accurate estimates of the scalp locations necessary to stimulate S1-index. This approach represents a clear goal for future work, and would be extremely useful for interpreting previous results and planning new studies (Xiao et al., 2018). Generating such a statistic will need to account for TMS coil size, shape, position, and orientation, intensity, waveform, frequency, and pattern; scalp-to-brain distance, cortical folding, and the size and function of the cortical area under study.

We have criticized the standard heuristic based on M1-FDI to locate S1-index, but our methods also rely on TMS over M1-FDI: the origin of our maps was M1-FDI; TMS intensity was set according to M1-FDI threshold. These practices are very common in TMS research, but we must be cautious about the circularity. There may be no reason why S1-index is best localized using M1-FDI as a reference, and no reason why parameters optimal for M1-FDI should be optimal for S1-index. Addressing this circularity is outside the present scope, but is important for future studies.

Recommendations for locating S1-index in transcranial stimulation studies

Depending on available equipment and funding, transcranial stimulation studies may need different methods to locate their targets. Ideally, neuronavigation with a recent high-resolution structural MRI and functional localizer will be used for each participant. Systematic review showed that very few studies met this ‘gold standard’ (Holmes & Tamè, in press). If individual fMRI is unavailable, individual MRI with group-level localizers or coordinates may suffice. The fMRI data need to be interpreted in conjunction with anatomical criteria. Registration of the participant’s head to the MRI needs to be done carefully; we recommend recording head and scalp measurements systematically - in one participant, we noticed scalp coordinates well outside other participants’; re-registering the MRI revealed that the wrong calibration file had been used, leading to ~3 cm coil positioning error. If a participant’s MRI is unavailable, then standard MRI templates, registered onto the participant’s scalp, provide only an approximate localization. The probabilistic central sulcus atlas we reported (Fig. 1B), suggests registration errors of several centimeters are likely. Without neuronavigation, scalp measurements using the 10:20 or 10:10 systems may be the only, very approximate, localization method. If the location of a target is estimated relative to that of primary motor cortex (i.e., using muscle twitches or motor-evoked potentials), or other functionally-defined locations, then researchers should use as many relevant sources of evidence to justify any heuristics used. Our work suggests that even very-commonly reported heuristics are not optimal for locating the intended target. Such heuristics may not be evidence-based.

534 **Conclusion**

535 More than a century after the first electrical stimulation of human somatosensory
536 cortex (Cushing, 1909), the accuracy of TMS coil positioning remains questionable.
537 The localization error in previous TMS studies of S1-hand is likely about 2.25 cm.
538 Evidence from the independent sources reported here converged on the finding that
539 S1-index is about 7-8 cm lateral to the vertex, or about 2 cm lateral and 0.5 cm
540 posterior to the scalp location for eliciting MEPs in the FDI muscle. These estimates
541 cannot be relied upon for any single participant – the range of scalp locations across
542 participants was 3-4 cm in each direction for each location. Multiple sources of
543 evidence for target location – probabilistic anatomy, group data, scalp measurements,
544 meta-analyses, and the gold standard of individual (F)MRI – should be sought in
545 every TMS study. To improve localization methods, we recommend systematic
546 reporting of participants' head sizes and all locations targeted, both along the scalp
547 and, if available, in MRI scanner/anatomical and standard (e.g., MNI152)
548 coordinates. The results of previous TMS studies targeting the index finger area of S1
549 need reassessment.

550 **References**

- 551 Balslev D, Christensen LOD, Lee J, Law I, Paulson OB, Miall RC. Enhanced
552 accuracy in novel mirror drawing after repetitive transcranial magnetic
553 stimulation-induced proprioceptive deafferentation. *J. Neurosci.* 24, 9698—
554 9702, 2004.
- 555 Barker AT, Jalilnous R, Freeston IL. Noninvasive magnetic stimulation of human
556 motor cortex. *Lancet* 1, 1106—1107, 1985.
- 557 Brainard DH. The psychophysics toolbox. *Spat Vis* 10, 433—436, 1997.
- 558 Chipchase LS, Schabrun SM, Cohen LG, Hodges PW, Ridding MC, Rothwell JC,
559 Taylor JL, Ziemann U. A checklist for assessing the methodological quality of
560 studies using transcranial magnetic stimulation to study the motor system: An
561 international consensus study. *Clin. Neurophysiol.* 123(9), 1698–1704, 2012.
- 562 Criswell E. *Cram's introduction to surface electromyography*. Jones and Barlett,
563 London, 2011.
- 564 Convento S, Rahman S, Yau JM. Selective attention gates the interactive crossmodal
565 coupling between perceptual systems. *Curr. Biol.* 28, 746—752, 2018.
- 566 Cowey A, Walsh VZ. Magnetically induced phosphenes in sighted, blind and
567 blindsighted observers. *NeuroReport* 11(14), 3269–3273, 2000.
- 568 Cushing H. A note upon the Faradic stimulation of the postcentral gyrus in conscious
569 patients. *Brain* 32, 44—54, 1909.
- 570 D'Amour S, Harris LR. Contralateral tactile masking between forearms. *Exp. Brain.*
571 *Res.* 232, 821—826, 2014.
- 572 Eickhoff SB, Stephan KE, Mohlberg H, Grefkes CB, Fink GR, Amunts K, Zilles K. A
573 new SPM toolbox for combining probabilistic cytoarchitectonic maps and

functional imaging data. *NeuroImage* 25(4): 1325–1335, 2005.

Enomoto H, Hanajima R, Yuasa K, Mochizuki H, Terao Y. Decreased sensory cortical excitability after 1 Hz rTMS over the ipsilateral primary motor cortex. *Clin. Neurophysiol.* 112, 2154—2158, 2001.

Fox PT, Narayana S, Tandon N, Sandoval H, Fox S, Kochunov PV, Lancaster JL. Column-based model of electric field excitation of cerebral cortex. *Hum. Brain Mapp.* 22, 1–16, 2004.

Geyer S, Schleicher A, Zilles K. Areas 3a, 3b, and 1 of human primary somatosensory cortex: Part 1. Micro structural organization and interindividual variabilities. *NeuroImage* 10, 63—83, 1999.

Holmes NP. The principle of inverse effectiveness in multisensory integration: Some statistical considerations. *Brain Topog.* 21, 168—176, 2009.

Holmes NP, Meteyard L. Subjective annoyance of TMS predicts reaction times differences in published studies. *Front. Psychol.* 9: 1989, 2018.

Holmes NP, Spence C, Hansen PC, Mackay CE, Calvert GA. The multisensory attentional consequences of tool use: A functional magnetic resonance imaging study. *PLoS ONE* 3, e3502, 2008.

Holmes NP, Tamè L. Multisensory perception: magnetic disruption of attention in human parietal lobe. *Curr. Biol.* 28, R259—261, 2018.

Holmes NP, Tamè L. Locating primary somatosensory cortex in human brain stimulation studies: Systematic review and meta-analytic evidence. *J. Neurophysiol.*, in press.

Jasper H. Report of the committee on methods of clinical examination in electroencephalography: 1957. *Electroencephalography Clin. Neurophysiol.* 10,

598 370—375, 1958.

599 Koessler L, Maillard L, Benhadid A, Vignal JP, Felblinger J, Vespignani H, Braun M.
600 Automated cortical projection of EEG sensors: Anatomical correlation via the
601 international 10–10 system. *NeuroImage* 46, 64—72, 2009.

602 Lagerlund TD, Sharbrough FW, Jack CR, Erickson BJ, Strelow DC, Cicora KM,
603 Busacker NE. Determination of 10 – 20 system electrode locations using
604 magnetic resonance image scanning with markers. *Electroencephalography*
605 *Clin. Neurophysiol.* 86, 7—14, 1993.

606 Lakens D, Adolffi F, Albers CJ, Anvari F, Apps MAJ, Argamon SE, Baguley T, Becker
607 RB, Benning SD, Bradford DE, Buchanan EM, Caldwell AR, Van Calster B,
608 Carlsson R, Chen S, Chung B, Colling LJ, Collins GS, Crook Z, Cross ES,
609 Daniels S, Danielsson H, DeBruine LM, Dunleavy DJ, Earp BD, Feist MI, Ferrell
610 JD, Field JG, Fox NW, Friesen A, Gomes C, Gonzalez-Marquez M, Grange JA,
611 Grieve AP, Grist J, Guggenberger R, van Harmelen A, Hasselman F, Hochard
612 KD, Hoffarth MR, Holmes NP, Ingre M, Isager PM, Isotalus HK, Johansson C,
613 Juszczak K, Kenny DA, Khalil AA, Konat B, Lao J, Larsen EG, Lodder GMA,
614 Lukavský J, Madan CR, Manheim D, Martin SR, Martin AE, Mayo DG, McCarthy
615 RJ, McConway K, McFarland C, Nio A, Nilsson G, de Oliveira CL, Orban de
616 Xivry J, Parsons S, Pfuhl G, Quinn KA, Marmolejo-Ramos F, Sakon JJ, Saribay
617 SA, Schneider IK, Selvaraju M, Sjoerds Z, Smith SG, Smits T, Spies J,
618 Sreekumar V, Steltenpohl CN, Stenhouse N, Świątkowski W, Vadillo MA, van
619 Assen MALM, Williams MN, Williams SE, Williams DR, Yarkoni T, Ziano I,
620 Zwaan RA. Justify Your Alpha: A Response to "Redefine Statistical
621 Significance". *Nat HumBehav* 2: 168–181, 2018.

622 Meteyard L, Holmes NP. TMS SMART – scalp mapping of annoyance ratings and
 623 twitches caused by transcranial magnetic stimulation. *J Neurosci Meth* 299: 34–
 624 44, 2018.

625 Nelson AJ, Chen R. Digit somatotopy within cortical areas of the postcentral gyrus in
 626 humans. *Cereb Cortex* 18(10): 2341–2351, 2008.

627 Niskanen E, Julkunen P, Säisänen L, Vanninen R, Karjalainen P, Könönen M. Group-
 628 level variations in motor representation areas of thenar and anterior tibial
 629 muscles: Navigated transcranial magnetic stimulation study. *Hum Brain Mapp*
 630 31(8): 1272–1280, 2010.

631 Okamoto M, Dan H, Sakamoto K, Takeo K, Shimizu K, Kohno S, Oda I, Isobe S,
 632 Suzuki T, Kohyama K, Dan I. Three-dimensional probabilistic anatomical cranio-
 633 cerebral correlation via the international 10–20 system oriented for transcranial
 634 functional brain mapping. *NeuroImage* 21(1): 99–111, 2004.

635 Oliveri M, Rossini PM, Filippi MM, Traversa R, Cicinelli P, Palmieri MG, Pasqualetti P,
 636 Caltagirone C. Time-dependent activation of parieto-frontal networks for
 637 directing attention to tactile space. A study with paired transcranial magnetic
 638 stimulation pulses in right-brain-damaged patients with extinction. *Brain* 123(9),
 639 1939–1947, 2000.

640 Petrov PI, Mandija S, Sommer IEC, van den Berg CAT, Neggers SFW. How much
 641 detail is needed in modeling a transcranial magnetic stimulation figure-8 coil:
 642 Measurements and brain simulations. *Public Library of Science ONE*,
 643 12(6):e178952, 2017.

644 Raffin E, Pellegrino G, di Lazzaro V, Thielscher A, Siebner HR. Bringing transcranial
 645 mapping into shape: Sulcus-aligned mapping captures motor somatotopy in

646 human primary motor hand area. *NeuroImage* 120: 164–175, 2015.

647 Reader AT, Tamè L, Holmes NP. Two instances of presyncope during magnetic
648 stimulation of the median nerve, and evaluation of resting motor threshold with
649 transcranial magnetic stimulation (TMS). *Open Science Framework*, 9 Oct.
650 2017. <https://osf.io/maurc/>

651 Rossi S, Hallett M, Rossini PM, Pascual-Leone A, The Safety of TMS Consensus
652 Group. Safety, ethical considerations, and application guidelines for the use of
653 transcranial magnetic stimulation in clinical practice and research. *Clin*
654 *Neurophysiol* 120(12): 2008–2039, 2009.

655 Rossini PM, Barker AT, Berardelli A, Caramia MD, Caruso G, Cracco RQ, Dimitrijevic
656 MR, Hallett M, Katayama Y, Lucking CH, Maertens de Nordhout AL, Marsden
657 CD, Murray NMF, Rothwell JC, Swash M, Tomberg C. Non-invasive electrical
658 and magnetic stimulation of the brain, spinal cord and roots: Basic principles
659 and procedures for routine clinical application. Report of an IFCN committee.
660 *Electroencephalography Clin Neurophysiol* 91(2-3): 79–92, 1994.

661 Rossini PM, Burke D, Chen R, Cohen LG, Daskalakis ZJ, Di Iorio R, di Lazzaro V,
662 Ferreri F, Fitzgerald PB, George MS, Hallett M, Lefaucheur J', Langguth B,
663 Matsumoto H, Miniussi C, Nitsche MA, Pascual-Leone A, Paulus WE, Rossi S,
664 Rothwell JC, Siebner HR, Ugawa Y, Walsh VZ, Ziemann U. Non-invasive
665 electrical and magnetic stimulation of the brain, spinal cord, roots and peripheral
666 nerves: Basic principles and procedures for routine clinical and research
667 application. An updated report from an I.F.C.N. committee. *Clin Neurophysiol*
668 126(6): 1071–1107, 2015.

669 Schweisfurth MA, Frahm J, Schweizer R. Individual fMRI maps of all phalanges and

670 digit bases of all fingers in human primary somatosensory cortex. *Front. Hum.*
671 *Neurosci.* 8, 2014.

672 Seyal M, Siddiqui I, Hundal NS. Suppression of spatial localization of a cutaneous
673 stimulus following transcranial magnetic pulse stimulation of the sensorimotor
674 cortex. *Electroencephal. Clin. Neurophysiol.* 105(1), 24–28, 1997.

675 Smith PL, Little DR. Small is beautiful: In defense of the small-n design. *Psychonom.*
676 *Bull. Rev.*, in press.

677 Sparing R, Hesse MD, Fink GR. Neuronavigation for transcranial magnetic
678 stimulation (TMS): Where we are and where we are going. *Cortex*, 46(1):118-
679 120, 2010.

680 Sugishita M, Takayama Y. Paraesthesia elicited by repetitive transcranial magnetic
681 stimulation of the postcentral gyrus. *NeuroReport* 4(5): 569–570, 1993.

682 Tamè L, Holmes NP. Involvement of human primary somatosensory cortex in
683 vibrotactile detection depends on task demand. *NeuroImage* 138: 184–196,
684 2016.

685 Tamè L, Moles AP, Holmes NP. Within, but not between hands interactions in
686 vibrotactile detection thresholds reflect somatosensory receptive field
687 organization. *Front Psychol* 5: 174, 2014.

688 Towle VL, Bolaños J, Suarez D, Tan KK, Grzeszczuk R, Levin DN, Cakmur R, Frank
689 SA, Spire JP. The spatial location of EEG electrodes: locating the best-fitting
690 sphere relative to cortical anatomy. *Electroencephalography Clin Neurophysiol*
691 86(1): 1–6, 1993.

692 Vitali P, Avanzini G, Caposio L, Fallica E, Grigoletti L, Maccagnano E, Villani F.
693 Cortical location of 10–20 system electrodes on normalized cortical MRI

694 surfaces. *Int J Bioelectromagn* 4(2): 147–148, 2002.

695 Watson AB, Pelli DG. QUEST: A Bayesian adaptive psychometric method. *Percept*

696 *Psychophys* 33(2): 113–120, 1983.

697 Xiao X, Yu X, Zhang Z, Zhao Y, Jiang Y, Li Z, Yang Y, Zhu C. Transcranial brain atlas.

698 *Sci. Adv.* 4(9): eaar6904, 2018.

699 Yoursy TA, Schmid UD, Alkadhi H, Schmidt D, Peraud A, Buettner A, Winkler PA.

700 Localization of the motor hand area to a knob on the precentral gyrus: A new

701 landmark. *Brain* 120(1): 141–157, 1997.

702 Zilles K, Kawashima RE, Dabringhaus A, Fukuda H, Schormann T. Hemispheric

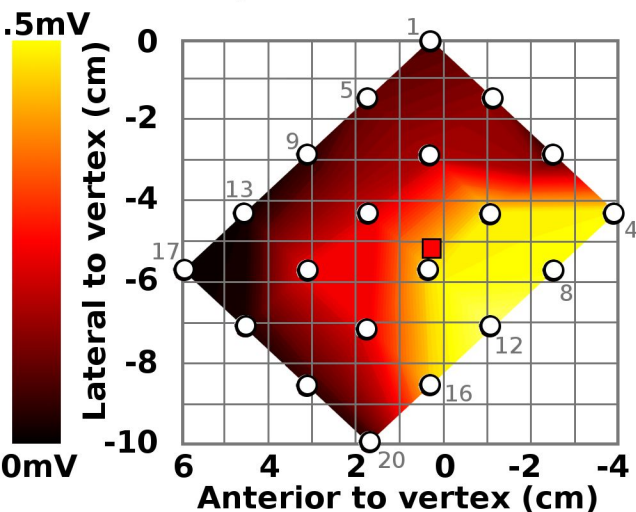
703 shape of european and japanese brains: 3-D MRI analysis of intersubject

704 variability, ethnical, and gender differences. *NeuroImage* 13(2): 262–271, 2001.

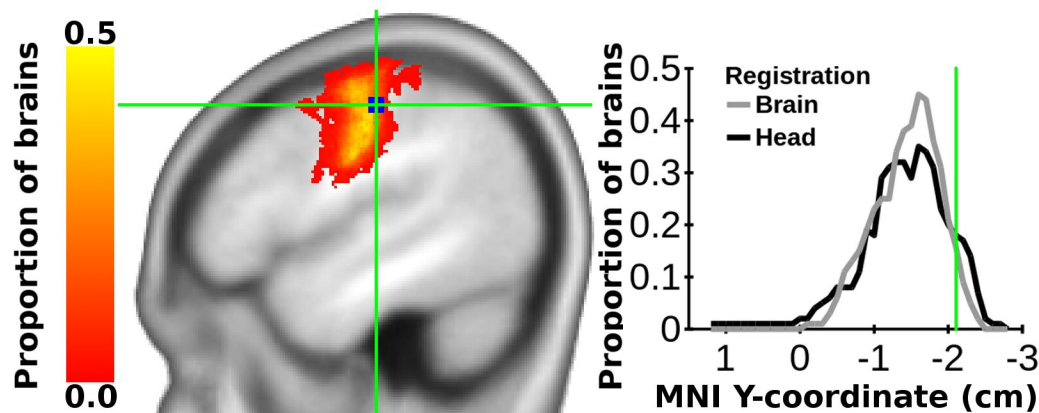
Fig. 1: Locating primary somatosensory cortex in human brain stimulation studies. Evidence for the scalp location of the primary somatosensory cortex representation of the right index finger (S1-index). All coordinates are in centimetres (cm) lateral to (i.e., left of) and anterior to (i.e., forward of) the vertex (Cz), or in MNI space. **A.** Mean motor evoked potential (MEP) amplitude during systematic mapping of the first dorsal interosseus muscle's primary motor cortex representation (M1-FDI) on the scalp in Experiment 2. Red square at Cz(-5.2,0.4): mean location of M1-FDI from all available studies conducted in the laboratory (N=56); white circles: locations tested. **B.** Probabilistic anatomy of the central sulcus, as estimated from 100 MRI scans. Colours on the brain scan represent the proportion of participants with central sulcus at that location. Blue square and green cross-hairs: mean reported MNI coordinate for the location of S1-index across 54 fMRI studies, MNI(-48,-21,50). The graph shows a cross-section along the MNI Y-axis for the selected coordinate. The range of likely central sulcus distances along this axis, after transformation of either the whole head (black), or the brain (grey), is 2-3 cm. **C.** TMS-related interference with tactile intensity discrimination (N=12, Auditory d' – Tactile d', t(11)-scores), is highest 7 cm lateral, and 0.76 cm anterior to the vertex. Thin black contour: uncorrected 1-tailed statistical significance (alpha) threshold ($p \leq .05$); thick black contour: alpha threshold Bonferroni corrected for 7 locations ($p \leq .007$); black 'target': maximum tactile interference; red square: M1-FDI; white circles: locations tested. **D.** Summary of all scalp locations ($M \pm SD$) studied in this report and those from a recent systematic review. Magenta circle: S1-index based on individual fMRI-guided TMS neuronavigation; yellow triangle: Mean C3 location on 101 participants' heads; open squares: estimated mean scalp location targeted for 43 TMS studies using M1-FDI as

729 a reference point (black); 16 TMS studies using M1-thenar as a reference point (mid
 730 grey); 21 TMS studies using hand movement as a reference point (light grey); black
 731 triangle: estimated mean scalp location targeted for 16 TMS studies using C3 as a
 732 reference point; black diamond: estimated mean scalp location of M1-FDI according
 733 to a meta-analysis. Black cross: mean location of maximum intensity discrimination
 734 thresholds in Experiment 1; black 'target': mean location of maximum difference
 735 between auditory and tactile intensity discrimination performance in Experiment 2. **E.**
 736 fMRI data. Re-analysis of FMRI data from Tamè and Holmes (2016): red-yellow
 737 shading shows the contrast between the right index finger versus all other fingers on
 738 the right hand. **F.** Mean tactile intensity discrimination thresholds for 9 participants in
 739 Experiment 1. White circles: locations tested. **G.** Mean \pm 95% confidence ellipsoids for
 740 M1-FDI (red) and S1-index (magenta) locations, as used by Tamè and Holmes
 741 (2016). **H.** Scalp landmarks used in the 10:20 electrode positioning system. White
 742 circle: vertex; green circles: other scalp landmarks and electrode positions, including
 743 C3', often positioned as indicated, at 2 cm posterior to C3, though likely located ~3.6
 744 cm posterior to C3.

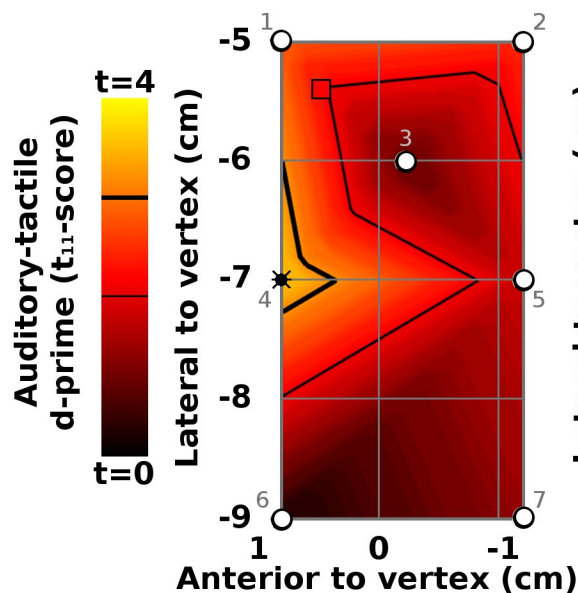
A. MEP map (E2)



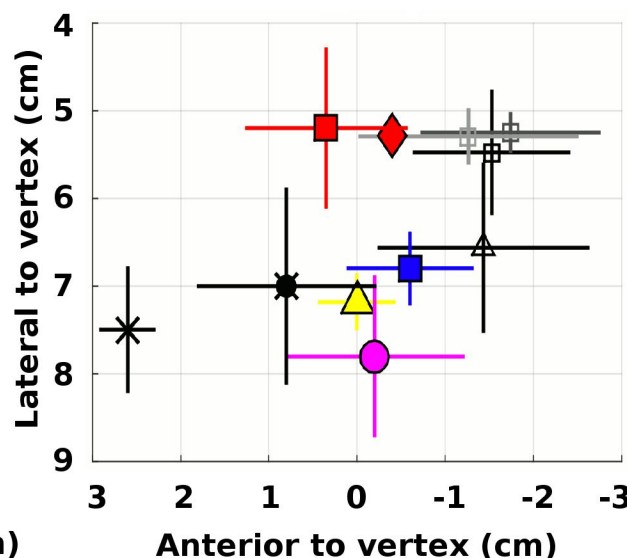
B. Probabilistic central sulcus anatomy



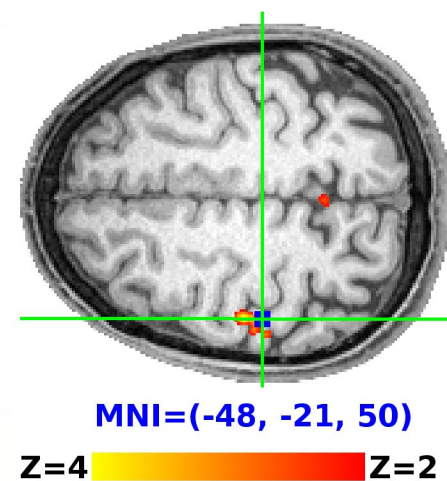
C. Tactile interference (E2)



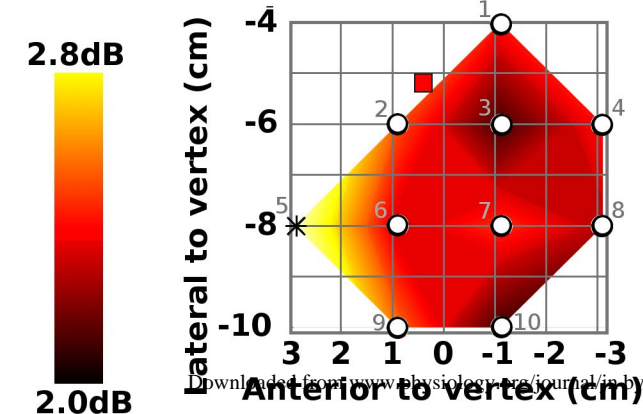
D. Mean \pm SD scalp positions



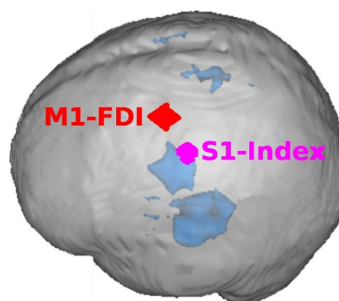
E. FMRI data



F. Tactile thresholds (E1)



G. TMS neuronavigation



H. Scalp anatomy

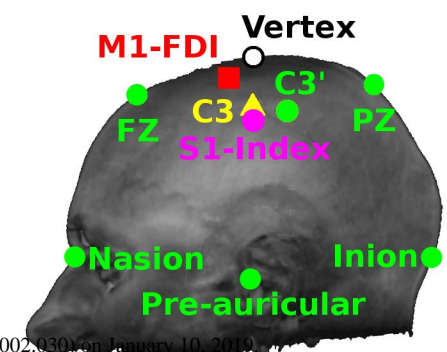


Table 1: Peak BOLD signal changes at the group level, to vibrotactile stimulation of left and right digits in 20 healthy participants

| Hand | Contrast | Digit | MNI | | | Z | Probabilistic anatomy (%) | | | | | | | |
|-------|--------------|-------|-----|-----|----|------|---------------------------|------|-----------------|----|----|----|----|----|
| | | | x | y | z | | Central gyri | | Brodmann's area | | | | | |
| | | | | | | | Pre | Post | 6 | 4a | 4p | 3b | 1 | 2 |
| Left | Differential | 1 | 56 | -12 | 46 | 3.43 | 20 | 57 | 9 | 41 | 1 | 32 | 82 | 17 |
| | | 2 | 48 | -12 | 54 | 3.77 | 42 | 27 | 47 | 38 | 0 | 8 | 43 | 0 |
| | | 3 | 42 | -20 | 54 | 2.41 | 32 | 32 | 15 | 41 | 13 | 66 | 19 | 0 |
| | | 4 | 42 | -22 | 62 | 2.83 | 28 | 34 | 49 | 38 | 0 | 21 | 55 | 0 |
| | | 5 | 40 | -30 | 64 | 1.34 | 5 | 47 | 7 | 35 | 8 | 31 | 76 | 0 |
| | Single | 1 | 56 | -12 | 48 | 5.32 | 19 | 52 | 7 | 44 | 0 | 22 | 76 | 10 |
| | | 2 | 50 | -14 | 56 | 4.39 | 17 | 50 | 26 | 18 | 0 | 0 | 37 | 0 |
| | | 3 | 46 | -22 | 60 | 4.08 | 9 | 48 | 9 | 10 | 0 | 19 | 96 | 3 |
| | | 4 | 40 | -30 | 66 | 4.1 | 5 | 58 | 14 | 38 | 6 | 12 | 65 | 0 |
| | | 5 | 40 | -30 | 64 | 3.36 | 5 | 47 | 7 | 35 | 8 | 31 | 76 | 0 |
| Right | Differential | 1 | -50 | -18 | 44 | 3.34 | 13 | 51 | 0 | 20 | 15 | 44 | 48 | 60 |
| | | 2 | -48 | -14 | 50 | 3.55 | 35 | 37 | 33 | 45 | 1 | 31 | 48 | 6 |
| | | 3 | -42 | -20 | 62 | 2.79 | 38 | 28 | 60 | 28 | 0 | 7 | 32 | 0 |
| | | 4 | -44 | -28 | 64 | 1.56 | 2 | 63 | 0 | 6 | 0 | 16 | 80 | 8 |
| | | 5 | -46 | -28 | 62 | 1.92 | 0 | 62 | 0 | 2 | 0 | 11 | 94 | 19 |
| | Single | 1 | -50 | -20 | 44 | 4.42 | 6 | 51 | 0 | 9 | 11 | 43 | 50 | 72 |
| | | 2 | -54 | -22 | 52 | 4.80 | 0 | 69 | 0 | 0 | 0 | 8 | 88 | 30 |
| | | 3 | -44 | -20 | 62 | 4.17 | 24 | 41 | 48 | 19 | 0 | 5 | 32 | 0 |
| | | 4 | -52 | -26 | 56 | 3.28 | 0 | 57 | 0 | 0 | 0 | 0 | 86 | 26 |
| | | 5 | -40 | -30 | 64 | 3.44 | 5 | 49 | 2 | 40 | 0 | 15 | 71 | 8 |

x: MNI x-coordinate in mm; y: MNI y-coordinate in mm; z: MNI z-coordinate in mm; Z: Z-score for the BOLD contrast; Post: postcentral gyrus; Pre: precentral gyrus. Probabilistic anatomy based on the Juelich probabilistic cytoarchitectural atlases viewed in FSL-view.

Data for the index finger are highlighted in bold text.

Table 2: Scalp locations of M1-FDI, S1-index, and C3/C4 relative to vertex (Cz), from seven independent sources of evidence

| Location and source | Location relative to vertex (Cz) mean±SD cm (min:max) | | | | | |
|--|--|--------------------------|------------------------|------------------|-----------------------|------------------------|
| | Left hemisphere | | | Right hemisphere | | |
| | N | Lateral | Anterior | N | Lateral | Anterior |
| M1-FDI, TMS studies (2011-18) | 56 | -5.2±0.8 (-7.0:-3.0) | 0.4±0.9 (-2.6:2.0) | 14 | 5.2±0.9 (3.5:7.5) | 0.5±0.9 (-1:1.8) |
| S1-index, TMS meta-analysis (N=96 studies, 1991-2017)* | 1693 | -5.9±0.9 (-8.2:-4.4) | -1.3±1.0 (-3.6:0.4) | - | - | - |
| C3/4, head measurements (2016-18) | 101 | -7.2±0.3 (-7.8:-6.6) | 0 | - | - | - |
| S1-index, FMRI meta-analysis (LH N=425; RH N=316, 54 studies, 1999-2017), projected onto scalp in MRI | 100 | -6.8±0.4 (-9.4:-5.7) | -0.6±0.7 (-2.3:2.2) | 100 | 6.9±0.4 (6.1:9.8) | -0.6±0.8 (-2.3:1.8) |
| S1-index, Experiment 1 (2014-15) | 10 | -7.5±0.7 (-9.0:-7.0) | 2.6±0.3 (2.0:3.0) | - | - | - |
| S1-index, Experiment 2 (2017) | 12 | -7.0±1.1 (-8.8:-5.2) | 0.8±1.0 (-1.5:2.1) | - | - | - |
| S1-index, FMRI study (N=20, 2012-14), group contrast projected onto scalp in navigated TMS studies (2016-18) | 11 | -7.8±0.9 (-10.0:-6.7) | -0.2±1.0 (-1.5:1.4) | 9 | 8.4±1.1 (7.0:10.3) | -0.4±0.6 (-1.1:0.3) |

* Collapsed across hemispheres, and using assumed scalp locations for M1-FDI/M1-APB

representations where not reported